Research Article

Cancer Immunology Research

Angiopoietin-2 as a Biomarker and Target for Immune Checkpoint Therapy

Xinqi Wu[1], Anita Giobbie-Hurder[2,3], Xiaoyun Liao[2,4], Courtney Connelly[2,4], Erin M. Connolly[2,5], Jingjing Li[1], Michael P. Manos[2], Donald Lawrence[6], David McDermott[7], Mariano Severgnini[2], Jun Zhou[1], Evisa Gjini[2], Ana Lako[2], Mikel Lipschitz[2], Christine J. Pak[2], Sara Abdelrahman[2], Scott Rodig[2,4], and F. Stephen Hodi[1,2,5]

Abstract

Immune checkpoint therapies targeting CTLA-4 and PD-1 have proven effective in cancer treatment. However, the identification of biomarkers for predicting clinical outcomes and mechanisms to overcome resistance remain as critical needs. Angiogenesis is increasingly appreciated as an immune modulator with potential for combinatorial use with checkpoint blockade. Angiopoietin-2 (ANGPT2) is an immune target in patients and is involved in resistance to anti-VEGF treatment with the monoclonal antibody bevacizumab. We investigated the predictive and prognostic value of circulating ANGPT2 in metastatic melanoma patients receiving immune checkpoint therapy. High pretreatment serum ANGPT2 was associated with reduced overall survival in CTLA-4 and PD-1 blockade–treated patients. These treatments also increased serum ANGPT2 in many patients early after treatment initiation, whereas ipilimumab plus bevacizumab treatment decreased serum concentrations. ANGPT2 increases were associated with reduced response and/or overall survival. Ipilimumab increased, and ipilimumab plus bevacizumab decreased, tumor vascular ANGPT2 expression in a subset of patients, which was associated with increased and decreased tumor infiltration by $CD68^+$ and $CD163^+$ macrophages, respectively. *In vitro*, bevacizumab blocked VEGF-induced ANGPT2 expression in tumor-associated endothelial cells, whereas ANGPT2 increased PD-L1 expression on M2-polarized macrophages. Treatments elicited long-lasting and functional antibody responses to ANGPT2 in a subset of patients receiving clinical benefit. Our findings suggest that serum ANGPT2 may be considered as a predictive and prognostic biomarker for immune checkpoint therapy and may contribute to treatment resistance via increasing proangiogenic and immunosuppressive activities in the tumor microenvironment. Targeting ANGPT2 provides a rational combinatorial approach to improve the efficacy of immune therapy. *Cancer Immunol Res; 5(1); 17–28. ©2016 AACR.*

Introduction

Recent developments in immune checkpoint therapy have changed the way patients with cancer are treated. Ipilimumab treatment, which targets CTLA-4, improves overall survival (OS) in patients with metastatic melanoma (1, 2). A phase I trial combining bevacizumab, a humanized monoclonal antibody targeting VEGF, with ipilimumab demonstrated favorable clinical activity compared with ipilimumab alone (3). Anti–PD-1 therapy with nivolumab or pembrolizumab, monoclonal antibodies that block interactions of PD-1 with PD-L1 and PD-L2, improve survival or have significant activity in a variety of cancer types, including metastatic melanoma, non–small cell lung cancer, renal cell cancer, bladder cancer, and Hodgkin disease (4–9). The combination of CTLA-4 and PD-1 blockade yields significantly longer progression-free survival and higher response rates than monotherapy in melanoma patients (10–12). Yet identification of biomarkers for predicting clinical outcomes to treatments and to search for mechanisms to overcome resistance are an unmet need.

Increasing evidence suggests that angiogenic factors play important roles in immune regulation and have immunoinhibitory activities (13). VEGF inhibits dendritic cell maturation and antigen presentation and tumor infiltration by lymphocytes, while promoting regulatory T cell (Treg) and myeloid-derived suppressor cell (MDSC) expansion in the tumor microenvironment (14–18). Higher pretreatment serum VEGF is associated with decreased survival in ipilimumab-treated metastatic melanoma patients (19). Angiopoietin-2 (ANGPT2), a ligand of the receptor tyrosine kinase Tie-2, functions as a vessel-destabilizing molecule and is a critical regulator of blood vessel maturation (20, 21). ANGPT2 is primarily produced by endothelial cells and facilitates angiogenesis. ANGPT2 is low in normal tissues but often highly upregulated in the tumor vasculature (22, 23). Elevated circulating ANGPT2 has been associated with poor

[1]Department of Medical Oncology, Dana-Farber Cancer Institute and Harvard Medical School, Boston, Massachusetts. [2]Center for Immuno-oncology, Dana-Farber Cancer Institute and Harvard Medical School, Boston, Massachusetts. [3]Department of Biostatistics and Computational Biology, Dana-Farber Cancer Institute, Boston, Massachusetts. [4]Department of Pathology, Brigham and Women's Hospital, Boston, Massachusetts. [5]Melanoma Disease Center, Dana-Farber Cancer Institute and Harvard Medical School, Boston, Massachusetts. [6]Massachusetts General Hospital Cancer Center, Boston, Massachusetts. [7]Beth Israel Deaconess Medical Center, Boston, Massachusetts.

Note: Supplementary data for this article are available at Cancer Immunology Research Online (http://cancerimmunolres.aacrjournals.org/).

Corresponding Author: F. Stephen Hodi, Dana-Farber Cancer Institute, 450 Brookline Avenue, Boston, MA 02215. Phone: 617-632-5053; Fax: 617-582-7992; E-mail: stephen_hodi@dfci.harvard.edu

doi: 10.1158/2326-6066.CIR-16-0206

prognosis and more invasive tumors in a variety of cancers, including melanoma (21–27). ANGPT2 can also play a role in inflammation (28, 29). Patients receiving immune therapy can make antibodies to ANGPT2 as the result of treatment (30). ANGPT2 can confer compensatory resistance to antiangiogenesis therapy targeting VEGF (29, 31–33), and high pretreatment serum ANGPT2 is associated with reduced response rate and survival in metastatic colorectal cancer patients receiving anti-angiogenesis therapy with bevacizumab (27). The possible prognostic/predictive role of ANGPT2 and its potential as a target for immune therapy requires further investigation.

The current study investigates the predictive and prognostic value of serum ANGPT2 concentrations for immune checkpoint therapy as well as investigating any synergistic effects of ANGPT2 on immune regulation. We found that high baseline circulating ANGPT2 concentrations, and early increases in ANGPT2 during treatment, were associated with shortened OS and/or reduced response rates. Immune checkpoint therapy elicited functional humoral immune responses to ANGPT2. Pathologic analyses revealed that immune checkpoint therapy increased or decreased the infiltration of tumor macrophages in association with elevated or reduced tumor vascular ANGPT2 expression. Additionally, ANGPT2 promoted PD-L1 expression on M2-polarized macrophages. These findings suggest serum ANGPT2 as a potential biomarker for predicting clinical outcomes to immune checkpoint therapy as well as a role for ANGPT2 in resistance to these therapies and possible target for synergistic combination treatments.

Materials and Methods

Tissue and blood collection

Patients with metastatic melanoma were treated and biospecimens were collected per Dana-Farber/Harvard Cancer Center Institutional Review Board (IRB)-approved protocols. Informed consent was obtained from all the patients involved in this study after the nature and possible consequences of the studies were explained. Patients with advanced melanoma enrolled in the phase I Ipi-Bev trial have been described previously (3). Demographics, disease status, and prior treatments of patients with metastatic melanoma receiving ipilimumab or PD-1 blockade treatment are summarized in Supplementary Table S1. For serum collection, blood samples collected in Vacutainer tubes with serum separator were centrifuged at 1,000× *g* for 15 minutes at room temperature, and the supernatant (serum) was collected and stored at ≤−20°C. For plasma collection, blood samples collected in Vacutainer tubes containing heparin were diluted with equal volume of RPMI1640 and subjected to Ficoll density gradient separation of PBMCs. The supernatant (plasma) above the PBMC layer was collected and stored at ≤−20°C.

Measurement of circulating ANGPT2

ANGPT2 in plasma/serum samples was measured using Magnetic Luminex Screening Assay kits (R&D Systems) per manufacturer's instructions.

Culture and treatment of endothelial cells and melanoma cells

Tumor-associated endothelial cells (TEC) were isolated using Dynabeads CD31 Endothelial Cell as guided by the manufacturer (Life Technologies) and confirmed by surface expression of CD31 and VEGFR2 and tube formation (34). HUVECs were purchased from Lonza. TECs and HUVECs were cultured in EGM-2 (Lonza). Melanoma cell lines K008, K033, and M23 were established approximately 25 years ago from harvested fresh tissues on Dana-Farber/Harvard Cancer Center IRB-approved protocols as described previously (35). Melanoma A375 cells were obtained from ATCC approximately 10 years ago. They were not authenticated but had confirmed expression of MITF and melanocytic markers. Melanoma cells were cultured in DMEM containing 10% FBS, penicillin (50 μg/mL), and streptomycin (100 μg/mL). In some experiments, EC and melanoma cells were cultured in a hypoxic chamber with 1% O_2. To examine the effect of VEGF and bevacizumab on ANGPT2 expression, EC and melanoma cells were incubated with VEGF (100 ng/mL; Cell Guidance Systems) and/or bevacizumab (25 μg/mL; Genetech) in serum and angiogenesis factor reduced EBM/EGM-2 (3:1, v/v) medium and DMEM containing 1% FBS, respectively. To examine the effect of enriched endogenous ANGPT2 antibodies on ANGPT2-mediated Erk1/2 phosphorylation, HUVECs were serum starved for 6 hours and treated with ANGPT2 (400 ng/mL; R&D Systems) preincubated with human normal IgG (Life Technologies) or enriched ANGPT2 antibodies (1.2 μg/mL) for 15 minutes at 37°C and 5% CO_2.

Generation and polarization of monocyte-derived macrophages

Frozen PBMCs isolated from healthy donors were thawed briefly at 37°C in a water bath, washed in R-PS [RPMI1640 containing 50 penicillin (μg/mL) and streptomycin (100 μg/mL)], and incubated in R-PS containing 5% FBS (R-PS5) on cell culture dishes for 1.5 hours. Floating cells were removed by washing with R-PS at least 5 times. The attached monocytes were cultured in R-PS10 medium (R-PS supplemented with 10% FBS) containing CSF1 (15–100 ng/mL; Biolegend) for 3 days to differentiate into macrophages. After being washed with R-PS, the attached monocyte-derived macrophages (MDM) were incubated with fresh R-PS10 containing CSF1 for 3 more days. MDMs were activated with CSF1 (100 ng/mL), IL4 (10 or 20 ng/mL; R&D Systems), or IL10 (10 or 20 ng/mL; R&D Systems) for 2 days. In some experiments, ANGPT2 (300 ng/mL; R&D Systems and EMD Millipore) was added to MDMs after 3 days of differentiation with CSF1 or when they were activated with IL4 or IL10 to examine its effect on PD-L1 expression. Phenotypes of polarized MDMs were analyzed by FACS after staining with APC-conjugated CD80 (Clone 2D-10; Biolegend) and PE-conjugated CD163 antibodies (Clone GHI/61; Biolegend).

Detection of PD-L1 expression on macrophages

MDMs were detached from culture dishes using Accutase (Life Technologies), incubated with FcR blocker (Miltenyi Biotec) for 30 minutes at 4°C, and stained with PE-conjugated PD-L1 antibody (Clone 29E.2A3; Biolegend) in PBS containing 1% BSA for 30 minutes at 4°C. In some experiments, macrophages were stained with FTIC-conjugated CD68 antibody (Clone FA-11; Biolegend) after PD-L1 staining and fixation/permeabilization. Macrophages were analyzed using FACS and the FlowJo software.

Detection of ANGPT2 antibodies in patient plasma samples

ANGPT2 antibodies in plasma samples were determined by immunoblot analysis and ELISA using recombinant human

ANGPT2 (R&D Systems). Immunoblot analysis of ANGPT2 antibodies with plasma samples was performed as previously described with minor modifications (3). Briefly, ANGPT2 was run in SDS gels and transferred onto PVDF membranes. After blocking with 5% BSA in PBS, the membranes were incubated overnight with paired pretreatment and posttreatment plasma samples diluted by 1×10^3 folds. Antibodies bound to ANGPT2 were detected with HRP-conjugated goat anti-human IgG antibody (Life Technologies) and visualized with ECL. For ELISA measurement of ANGPT2 antibodies, recombinant human ANGPT2 was coated in TBS onto 96-well plates overnight. The plates were rinsed and blocked with a protein-free blocking solution (Thermo Scientific) for 1.5 hours at room temperature. Plasma samples were diluted by 500- to 2,000-fold in the blocking solution containing 0.1% Tween-20 and incubated with coated ANGPT2 for 1 hour at 4°C. Wells coated with His tag were used as background controls (named as "His Tag" background). To make sure signals were from plasma antibodies, additional wells coated with ANGPT2 and incubated with the Tween-20 containing blocking solution without plasma were also included (named as "No Plasma" background). The plates were washed extensively with PBST (PBS plus 0.05% Tween-20) and incubated with diluted rabbit F(ab')2 HPR anti-human IgG (SouthernBiotech) for 1 hour at room temperature. The plates were washed thoroughly with PBST and incubated with diluted biotinyl-tyramide (PerkinElmer) for 15 minutes at room temperature. After another thorough washing with PBST, the plates were incubated with streptavidin-HRP diluted in PBST plus 1% BSA for 30 minutes at room temperature. The plates were washed thoroughly with PBST and developed with TMB. OD at 450 and 570 nm was recorded using a microplate reader. Antibody titer was calculated by subtracting OD 570 from OD 450 and subtracting "His Tag" background and "No Plasma" background from ANGPT2 reading.

Purification of ANGPT2 antibodies from plasma

Recombinant human ANGPT2 (6 μg) was coupled to activated NHS magnet beads (40 μL; Thermo Scientific). Plasma samples (600 μL) were diluted with equal volume of PBS and incubated with the ANGPT2-coupled beads with rotation at 4°C overnight. The beads were pulled down with a magnet and washed with PBS 5 times. The antibodies bound to ANGPT2 were eluted with 0.1 mol/L glycine (pH 2.5) from the beads and neutralized with 1/10 volume of 1 mol/L Tris-Cl (pH 9.0). The antibodies were concentrated using an Amicon Ultra filter and stored in PBS supplemented with 0.02% BSA at 4°C. IgG content was determined by ELISA against normal human IgG (Life Technologies).

Immunohistochemical (IHC) staining

For IHC staining of ANGPT2 and CD163, 5-μm-thick paraffin-embedded sections were pre-baked at 60°C for 1 hour, deparaffinized, and rehydrated. Antigen retrieval was induced by heating sections in citrate buffer (pH 6.0, Invitrogen) for 30 minutes using a steamer. After cooling for 30 minutes, sections were treated with peroxidase block (DAKO) for 5 minutes, followed by serum-free protein block (DAKO) for 20 minutes. Slides were then incubated overnight at 4°C with primary antibodies against ANGPT2 (1:25, sc-74403; Santa Cruz Biotechnology) or CD163 (1:200, 10D6; NeoMarkers) diluted in Da Vinci Green Diluent (Biocare Medical). For secondary reagents, Envision anti-mouse HRP-labeled polymer (DAKO) was applied for 30 minutes to sections for CD163 staining. ANGPT2 sections were incubated with Novocastra Post Primary (Leica Biosystems) for 30 minutes, followed by Novolink Polymer (Leica Biosystems) for 30 minutes. Sections were then developed with diaminobenzidine (DAKO), counterstained with hematoxylin, dehydrated, and mounted. CD68 (PG-M1; DAKO) staining was performed using an automated staining system (Bond III; Leica Biosystems) following the manufacturer's protocols for the Bond Polymer Refine detection system (Leica Biosystems). Heat-induced antigen retrieval was performed using ER1 solution (pH 6.0; Leica Biosystems) for 30 minutes. Anti-CD68 antibody was diluted 1:200 in Da Vinci Green Diluent and incubated for 30 minutes. Slides were removed from the autostainer to be dehydrated and mounted. ANGPT2 expression was observed in cytoplasm of tumor cells and endothelia of small blood vessels. The expression was considered positive if $\geq$10% of cells had cytoplasmic staining. The intensity and the percentage of positive stained cells were assessed and recorded separately. Scoring was performed twice with a 1-week interval. For CD163 and CD68 staining, all slides were scanned using the Aperio Scan Scope (Aperio Technologies). After saving of each digital image, one to five representative areas of tumor (excluding areas of necrosis, artifact and other poor quality regions) were selected for analysis. Aperio ImageScope software (Aperio) was used, including a positive pixel count algorithm. Average percentage of area for positive staining was recorded as a final result for each case. All the slides were evaluated and scored by a pathologist (X. Liao) blinded to clinical data.

Immunoblot analyses

Cells were lysed in 1× lysis buffer (Cell Signaling Technology) supplemented with proteinase inhibitor cocktail (Roche), and centrifuged for 10 minutes at 14,000 rpm. Supernatants were collected, run on SDS gels, and transferred onto membranes. The membranes were blocked and probed with ANGPT2 antibody (Clone F-1; Santa Cruz Biotechnology), Erk1/2 antibody, or pErk1/2 antibody (Cell Signaling Technology). Representative results from one of the two experiments are shown.

Statistical analysis

The algorithm of Contal-O'Quigley (36) was used to estimate the optimal division points of pretreatment ANGPT2 and fold changes in ANGPT2. This algorithm divides the sample into high and low based on all possible values of pretreatment ANGPT2 (or ANGPT2 fold change) and assesses OS based on the resulting two categories. The division point with the largest log-rank statistic was considered to be the "best" division point for the respective ANGPT2 measurement. OS was defined as the time from trial enrollment to death from any cause. The survival distribution was summarized using the method of Kaplan–Meier; confidence intervals (CI) were estimated using log (−log (survival)) methodology. To address the potential for guarantee–time bias, three-month conditional landmark analyses were used to explore the relationship between fold change in ANGPT2 and survival. Patients who were alive and had pretreatment and subsequent ANGPT2 measurements within 3 months were followed forward in time. Cox proportion hazards models were used to describe the relationship between ANGPT2 categories and response or survival. Cox models were stratified by trial (ipilimumab, ipilimumab plus bevacizumab, PD-1 blockade) to allow for differences between trials in the baseline hazard of death. Hazard ratios are shown with 95% CIs. Statistical significance of Cox model results is

based on the Wald test. The association between pretreatment serum ANGPT2 levels or ANGPT2 fold changes and clinical responses, and the association between immune therapy and serum ANGPT2 changes, were evaluated using Fisher exact tests. The correlation between immune therapy and serum ANGPT2 fold changes was evaluated using the Kruskal–Wallis test. Holm–Bonferroni correction was used to preserve overall 0.05 type-1 error for multiple comparisons. $P < 0.05$ was considered statistically significant for all comparisons.

Results

Patients

A total of 48, 43, and 43 patients with advanced melanoma on immune checkpoint therapy with ipilimumab, ipilimumab plus bevacizumab, or PD-1 blockade, respectively, were analyzed for serum ANGPT2 concentrations before and during treatment. Patients enrolled in the phase I ipilimumab plus bevacizumab trial have been described previously (3). Demographics, disease status, and prior treatment of the patients on ipilimumab or PD-1 blockade treatment are summarized in Supplementary Table S1. Approximately 16.7%, 19.6%, and 37.2% of patients on ipilimumab, ipilimumab plus bevacizumab, or PD-1 blockade treatment, respectively, achieved complete or partial responses. In addition, 33.3%, 47.8%, and 25.6% of them had stable disease. The median follow-up time in the current dataset for all data combined was 33 months (95% CI, 22–40).

Poor survival in ANGPT2-high patients receiving ipilimumab alone or with bevacizumab

To determine if pretreatment serum ANGPT2 levels were associated with clinical outcomes, the patients were divided into two groups, based on their pretreatment serum concentrations of ANGPT2. The division point was determined using the Contal–O'Quigley algorithm (36) and found to be 3,175 pg/mL for all three groups of patients combined. High (>3175 pg/mL) or low (≤3175 pg/mL) pretreatment ANGPT2 concentrations were not associated with pretreatment lactose dehydrogenase (LDH) concentrations, gender, or stage of pooled patients receiving ipilimumab or ipilimumab plus bevacizumab (Supplementary Table S2). The median OS of patients with high or low pretreatment serum ANGPT2 was 12.2 (95% CI, 5.7–∞) versus 28.2 (95% CI, 13.5–∞) months ($P = 0.165$), respectively, for patients treated with ipilimumab alone (Supplementary Fig. S1A). High pretreatment serum ANGPT2 was associated with reduced OS also in patients treated with ipilimumab plus bevacizumab [median survival (high vs. low): 10.9 (95% CI, 3.1–19.8) vs. 19.3 (95% CI, 16.1–∞) months, $P = 0.0125$; Supplementary Fig. S1B]. This pattern held when data from patients treated with either ipilimumab or ipilimumab plus bevacizumab were pooled [10.9 (95% CI, 6–20) vs. 19.7 (95% CI, 16–55) months, $P = 0.004$; Fig. 1A]. In the ipilimumab plus bevacizumab treated patients, none of the 10 with high serum ANGPT2 achieved complete or partial remissions, whereas 8 out of the 33 (24.2%) with low ANGPT2 did. For ipilimumab alone, patients with low or high pretreatment ANGPT2 levels had similar response rates (17.6% vs. 16.1%).

Reduced OS associated with ipilimumab-induced early increases of serum ANGPT2

To examine whether dynamic changes in serum ANGPT2 were associated with treatment outcomes, posttreatment samples collected within 3 months after treatment initiation were analyzed. The division point for fold change of serum ANGPT2 within this time frame was 1.25 in all patients combined, as determined using the Contal–O'Quigley algorithm. The median OS of ipilimumab-treated patients based on this cutoff (≥1.25 vs. <1.25) was 12.4 (95% CI, 5–55) versus 28.1 (95% CI, 14–∞) months ($P = 0.019$; Supplementary Fig. S1C). Ipilimumab plus bevacizumab-treated patients with fold changes ≥ 1.25 also had shortened OS (10.9 months, 95% CI, 5–∞) compared with those with fold changes < 1.25 (18.0 months, 95% CI, 14–∞), although this did not reach statistical significance due to small number of patients ($n = 4$) with fold changes ≥ 1.25 ($P = 0.59$; Supplementary Fig. S1D). ANGPT2 increases were significantly associated with reduced OS when data from patients receiving ipilimumab or ipilimumab plus bevacizumab were pooled [median survival: 12.2 (95% CI, 5–55) vs. 19.3 (95% CI, 16–35) months, $P = 0.02$; Fig. 1B]. All patients treated with ipilimumab or ipilimumab plus bevacizumab with ANGPT2 increases of at least 25% had either stable disease or progressive disease, except for one ipilimumab-treated patient with a 26.5% ANGPT2 increase who achieved a partial response (Fig. 1C).

Reduced OS in ANGPT2-high patients treated with PD-1 blockade

Among the PD-1 blockade-treated patients, 34 had low and 9 had high pretreatment serum ANGPT2. High or low pretreatment ANGPT2 was not associated with patient characteristics except for LDH concentrations (Supplementary Table S2). High pretreatment serum ANGPT2 was significantly associated with reduced OS ($P = 0.004$; Fig. 1D). The median OS of patients with high pretreatment ANGPT2 was 7.3 (95% CI, 3.4–25.9) months, whereas that of patients with low pretreatment ANGPT2 was not reached because more than half of the patients were still alive. Patients with high or low pretreatment ANGPT2 had comparable response rates (33.3% and 38.2%, respectively).

Reduced response to PD-1 blockade if early increases of serum ANGPT2 were induced

Forty-three PD-1 blockade-treated patients with posttreatment samples collected within a 3-month time frame were analyzed for association of ANGPT2 fold changes and clinical outcomes. Patients with progressive (PD) and stable disease (SD) had significantly larger ANGPT2 fold changes than patients with partial responses (PR; PR vs. PD, $P = 0.007$; PR vs. SD, $P = 0.002$; SD vs. PD, $P = 0.87$; Supplementary Fig. S2A). Fold changes were significantly associated with clinical responses ($P = 0.002$), and small fold changes were significantly associated with a higher response rate (58% vs. 6%; Fig. 1E). Similar to ipilimumab-treated patients, all patients with ANGPT2 fold change ≥ 1.25 had SD or PD, except one patient with an ANGPT2 fold change of 1.25 who achieved PR (Fig. 1F). ANGPT2 increases also appeared to be associated with reduced OS [median survival 16.3 (95% CI, 6.8–∞) vs. 36.7 (95% CI, 13.7–∞) months; Supplementary Fig. S2B], although it did not reach statistical significance ($P = 0.22$).

High initial serum ANGPT2, then therapy-induced increase, predicts poor OS and PD

We next investigated whether the combination of pretreatment serum ANGPT2 concentrations and the fold change after

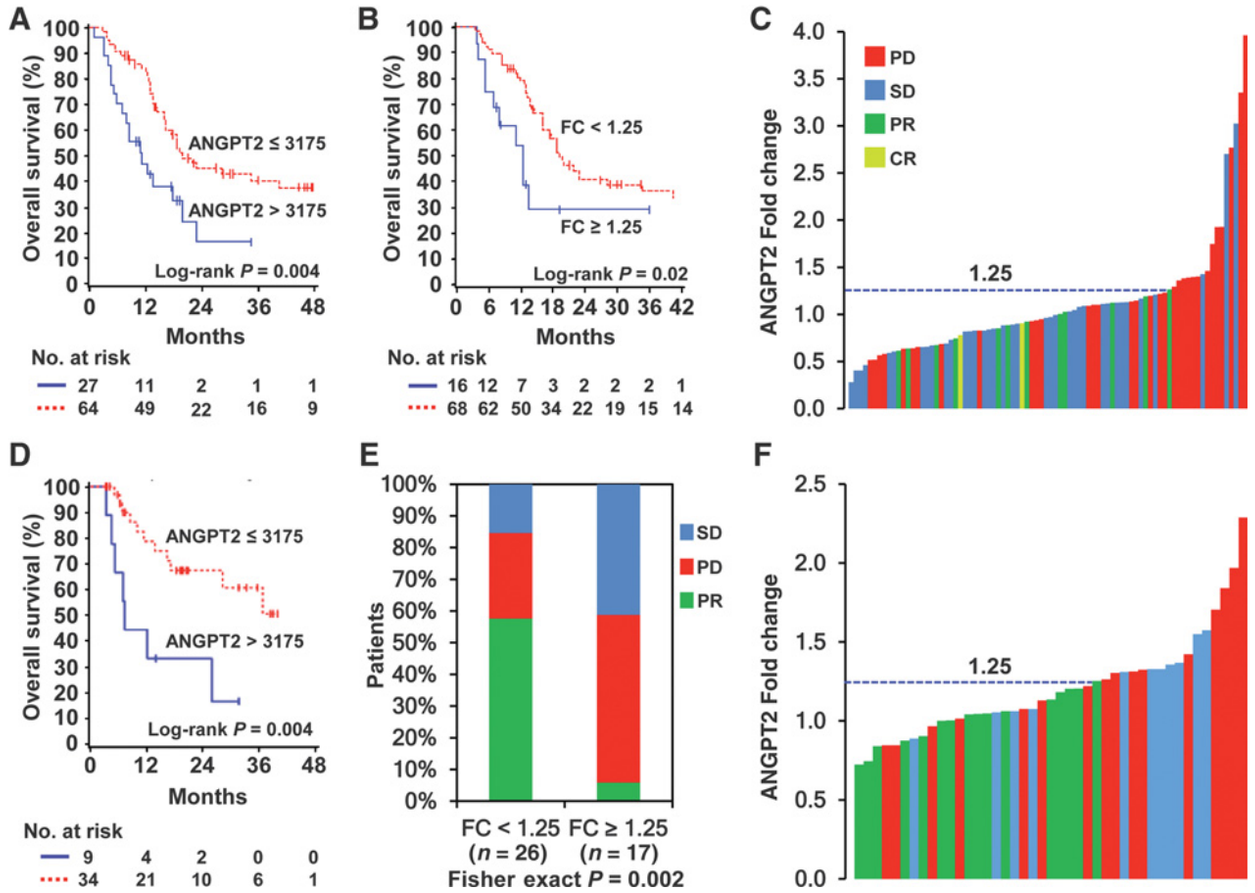

Figure 1.

High pretreatment ANGPT2 concentrations and increases in serum ANGPT2 were associated with poor clinical outcomes to immune checkpoint therapy in metastatic melanoma. **A** and **B,** Kaplan–Meier survival curves of pooled data from patients receiving ipilimumab or ipilimumab plus bevacizumab, based on ANGPT2 pretreatment concentrations (**A**, $n = 91$) and fold changes (**B**, $n = 84$)**. C,** ANGPT2 fold changes and clinical responses in pooled patients receiving ipilimumab or ipilimumab plus bevacizumab ($n = 84$). Each bar represents a patient and its color indicates clinical response of the patient. **D,** Kaplan–Meier survival curves of PD-1 blockade–treated patients by pretreatment ANGPT2 levels ($n = 43$). **E,** Proportions of PD-1 blockade–treated patients with PR, SD, and PD by ANGPT2 fold changes ($n = 43$). **F,** ANGPT2 fold changes and clinical responses to PD-1 blockade ($n = 43$).

immune checkpoint therapy would enhance the predictive power of serum ANGPT2. To do this, we combined datasets of all three groups of patients. High pretreatment ANGPT2 was associated with reduced OS in the pooled data [median survival: 10.9 (95% CI, 6.8–17.6) vs. 28.2 (95% CI, 18.6–∞) months, $P < 0.0001$; Fig. 2A]. The hazard ratio estimated from the Cox model stratified by trial is 2.48 (95% CI, 1.5–4.1; $P = 0.0003$). In addition, large ANGPT2 fold changes were associated with shortened OS [median survival: 12.4 (95% CI, 7.9–54.8) vs. 22.9 (95% CI, 17.6–40.6) months, $P = 0.002$; Fig. 2B]. ANGPT2 fold changes were also significantly associated with clinical response ($P = 0.001$; Fig. 2C), and response was significantly higher among patients with fold change < 1.25 (<1.25 vs. ≥1.25, 29.8% vs. 6.1%). Furthermore, the combination of pretreatment ANGPT2 serum concentrations and fold changes was associated with OS ($P = 0.001$; Fig. 2D). Patients with high pretreatment ANGPT2 and large fold changes had the worst survival, whereas those with low pretreatment ANGPT2 and small fold changes had the best survival [median survival 7.9 (95% CI, 3.8–∞) vs. 34.6 (95% CI, 18.7–∞) months]. Patients with high pretreatment ANGPT2 and small fold changes or low pretreatment and large fold changes had intermediate survival [13.6 (95% CI, 7.3–22.9) and 16.3 (95% CI, 10–54.8) months, respectively]. The combination of pretreatment ANGPT2 and fold changes was also significantly associated with clinical responses ($P = 0.006$; Fig. 2E). One of the 11 patients (9.1%) with high pretreatment ANGPT2 and large fold changes achieved PR/CR, in comparison with 23 of the 72 patients (31.9%) with low pretreatment ANGPT2 and small fold changes ($P = 0.002$). In contrast, 9 of the 11 patients (81.8%) with high pretreatment ANGPT2 and large fold changes had PD compared with 20 of the 72 patients (27.8%) with low pretreatment ANGPT2 and small fold changes. Patients with low pretreatment ANGPT2 and large ANGPT2 fold changes also had a low response rate (4.6%) than patients with low pretreatment ANGPT2 and small fold changes ($P = 0.01$). Patients with low pretreatment ANGPT2 and large ANGPT2 fold changes or high pretreatment ANGPT2 and small fold changes had intermediate progression rates (54.5% and 36.4%, respectively). These observations suggest

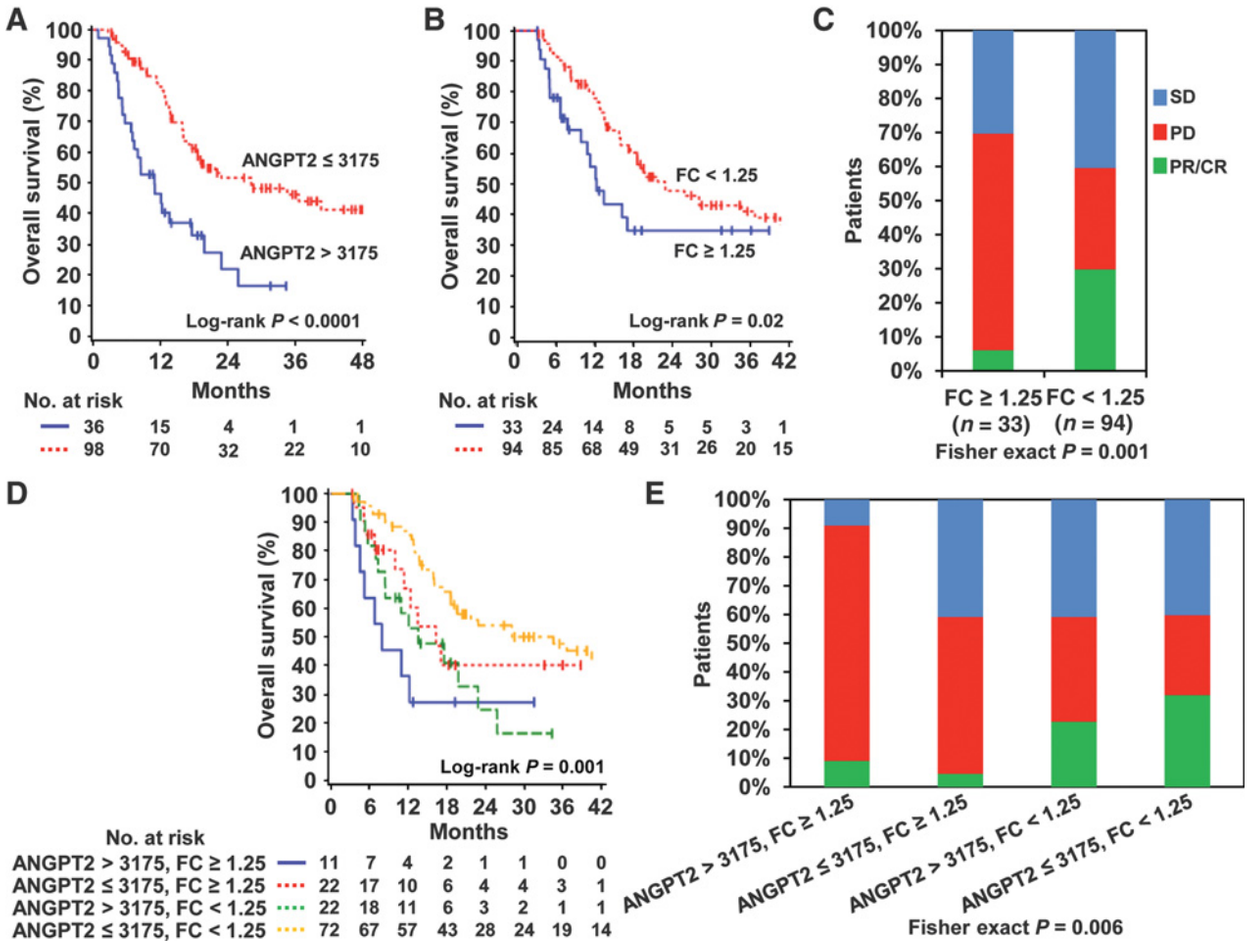

Figure 2.

High pretreatment serum ANGPT2 concentrations followed by treatment-induced increases were associated with the worst OS and progressive disease. Data sets from patients receiving ipilimumab, ipilimumab plus bevacizumab or PD-1 blockade were combined and analyzed. **A,** Kaplan–Meier survival curves based on pretreatment ANGPT2 levels ($n = 134$). **B,** Kaplan–Meier survival curves by ANGPT2 fold changes ($n = 127$). **C,** Proportions of patients with complete remission/partial remission (CR/PR), stable disease (SD) and progressive disease (PD) according to ANGPT2 fold changes ($n = 127$). **D,** Kaplan–Meier survival curves based on pretreatment ANGPT2 concentrations and fold changes ($n = 127$). **E,** Proportions of patients with CR/PR, SD, and PD by the combination of pretreatment ANGPT2 levels and fold changes ($n = 127$).

that the combination of high pretreatment serum ANGPT2 and large fold change following the initiation of treatment is a stronger predictor for PD and poor OS than either alone.

Immune checkpoint therapy influenced serum ANGPT2 concentrations

We next compared the effects of ipilimumab, ipilimumab plus bevacizumab, and PD-1 blockade on circulating ANGPT2. We found that the effect of ipilimumab plus bevacizumab on serum ANGPT2 was significantly different from that of ipilimumab and PD-1 blockade ($P = 0.0001$; Fig. 3A). Although 7.1%, 30.9%, and 39.5% of patients receiving ipilimumab plus bevacizumab, ipilimumab, and PD-1 blockade, respectively, displayed an increase in serum ANGPT2 by 25% or more, 38.1%, 16.7%, and 4.6% of patients, respectively, displayed a decrease by at least 25% within 3 months after treatment initiation (Fig. 3A). Furthermore, ipilimumab plus bevacizumab-treated patients displayed smaller ANGPT2 fold changes than ipilimumab and PD-1 blockade-treated patients ($P = 0.0001$; Fig. 3B; Supplementary Table S3).

Bevacizumab blocked VEGF-induced tumor vascular ANGPT2 expression

To further address the effect of bevacizumab on ANGPT2 expression, we examined ANGPT2 expression in cultured TECs and tumor cells (detailed protocols are described in Materials and Methods), as well as in paired pretreatment and posttreatment tumor biopsies from patients treated with ipilimumab or ipilimumab plus bevacizumab. Bevacizumab decreased ANGPT2 expression in TEC after 96 hours (Fig. 3C). VEGF enhanced ANGPT2 expression in TEC under normoxic and hypoxic conditions, while bevacizumab blocked VEGF-induced ANGPT2 expression (Fig. 3D). In melanoma cells, hypoxia increased ANGPT2 expression, whereas VEGF appeared to have no or minimal inhibitory effects (Supplementary Fig. S3). Among 5 ipilimumab-treated patients whose tumors were analyzed, ANGPT2

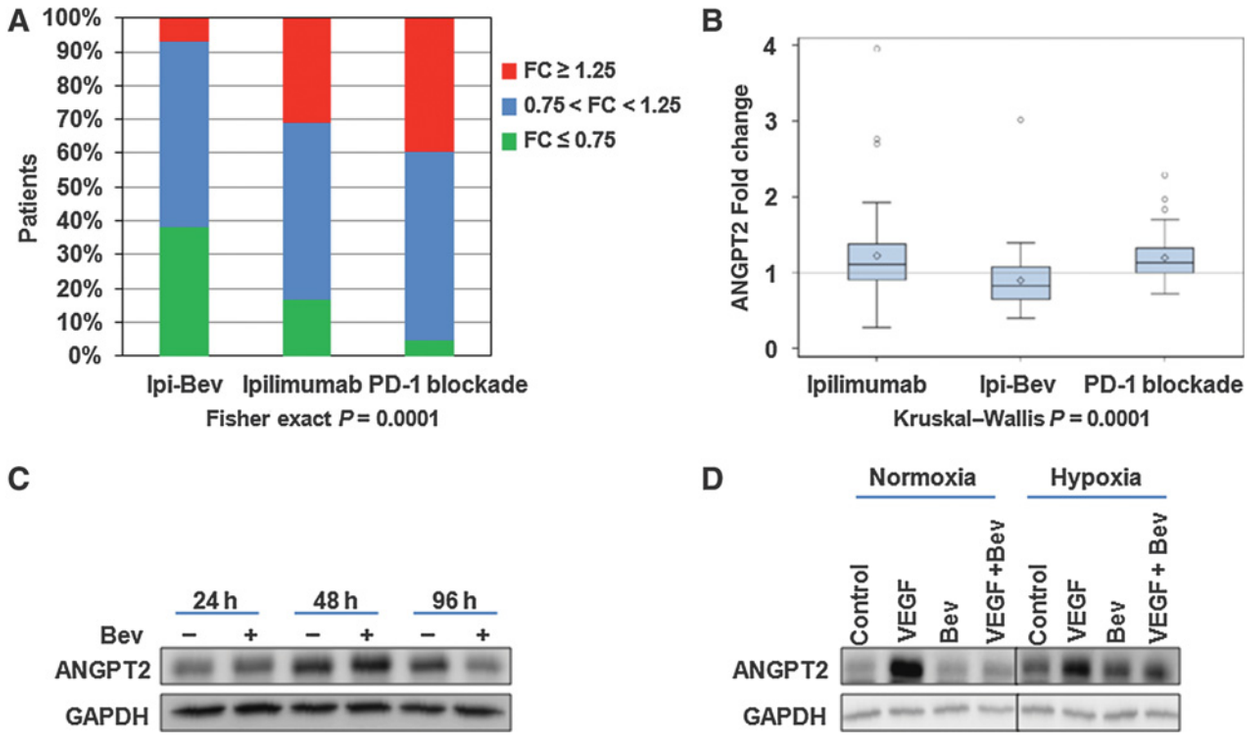

Figure 3.

PD-1 blockade and ipilimumab increased, whereas ipilimumab plus bevacizumab (Ipi-Bev) decreased serum ANGPT2 in significant proportions of patients. **A,** Proportions of patients displayed increase (fold change $\geq$ 1.25), decrease (fold change $\leq$ 0.75) or no change (0.75 < fold change < 1.25) in ANGPT2 in response to immune checkpoint therapy. **B,** Ipilimumab plus bevacizumab-treated patients (n = 43) displayed smaller fold changes than patients receiving ipilimumab (n = 41) or PD-1 blockade (n = 43). The diamonds, horizontal lines, and upper and lower boundaries of the boxes represent the sample average, median, 75th and 25th percentiles, respectively. **C,** Bevacizumab (Bev) downregulated ANGPT2 expression in TEC. **D,** VEGF promoted ANGPT2 expression and bevacizumab blocked VEGF-induced ANGPT2 expression in TEC. Representative images of two experiments are shown.

was barely detected in the pretreatment tumors but highly expressed in both tumor cells and endothelia of posttreatment tumors in two of them (Fig. 4A; Ipi-P1 and Ipi-P2; Supplementary Table S4). Another ipilimumab-treated patient also displayed increased ANGPT2 expression in endothelial cells but not in melanoma cells in posttreatment biopsies (Ipi-P3; Supplementary Table S4). In comparison, ANGPT2 expression was significantly decreased in tumor vessels of the posttreatment biopsies of 2 patients among the 7 ipilimumab plus bevacizumab-treated patients analyzed (Fig. 4B; P1 and P28; Supplementary Table S4). Our *in vitro* and *in vivo* findings support the inhibitory effect of bevacizumab on VEGF-induced ANGPT2 expression in tumor-associated endothelia. Nonetheless, ANGPT2 expression in response to ipilimumab and ipilimumab plus bevacizumab is heterogeneous, with modest decreases (Ipi-P4), increases (P20 and P27), or no change (P4, P9, and P31) in its expression having also been observed (Fig. 4C; Supplementary Table S4). This may reflect heterogeneity in the tumor microenvironment and the complex regulation of ANGPT2 expression in tumors by multiple factors (23).

Tumor vascular ANGPT2 was associated with macrophage infiltration

Given the known expression of Tie-2 (ANGPT2 receptor) on monocytes/macrophages (37, 38), we next asked if the addition of bevacizumab to ipilimumab treatment resulting in decreased ANGPT2 expression had an impact on tumor macrophage infiltration. Examination of the tumors from ipilimumab-treated patients with robust ANGPT2 induction revealed an increase in $CD68^+$ and $CD163^+$ macrophages as a function of treatment (Fig. 4A; Supplementary Table S4). Similarly, we observed increased infiltration of $CD68^+$ and $CD163^+$ macrophages in the posttreatment tumor biopsies of the ipilimumab plus bevacizumab patients with increased vascular ANGPT2 expression (Fig. 4C; Supplementary Table S4). In contrast, substantially fewer $CD68^+$ and $CD163^+$ macrophages were detected in posttreatment biopsies where ANGPT2 was significantly downregulated in both tumor cells and TECs (Fig. 4B). Additional paired biopsy analyses revealed that changes in tumor $CD68^+$ and/or $CD163^+$ macrophage infiltration overall correlated with changes in tumor endothelial ANGPT2 expression: increased $CD68^+$ and/or $CD163^+$ macrophages were observed in three of the four cases with elevated vascular ANGPT2 expression in the posttreatment biopsies (Supplementary Table S4; Fig. 4D), while decreased $CD68^+$ and $CD163^+$ macrophages were detected in three of the three cases with reduced vascular ANGPT2 expression in the posttreatment biopsies (Supplementary Table S4; Fig. 4E). Nonetheless, increased and decreased macrophage infiltration was also observed in cases where vascular ANGPT2 was not altered

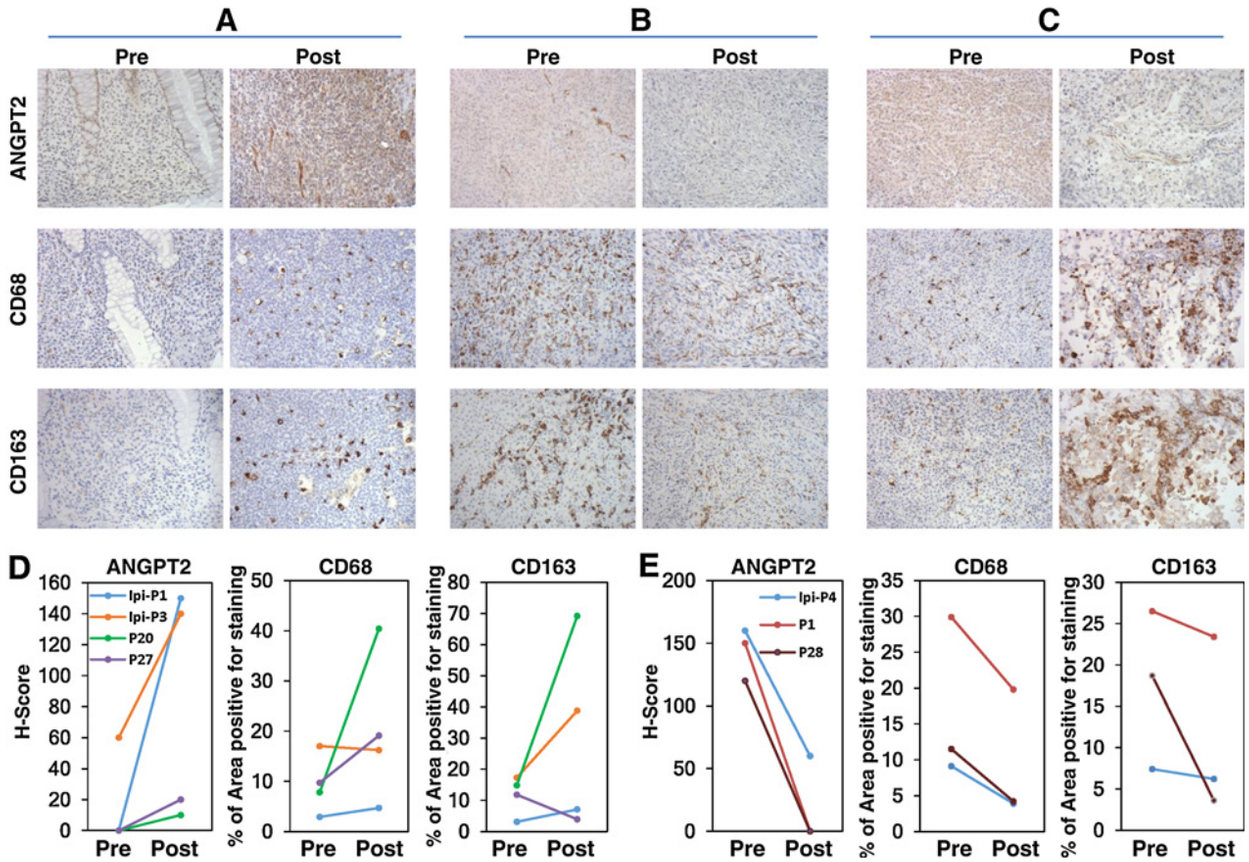

Figure 4.

Ipilimumab and ipilimumab plus bevacizumab influenced tumor ANGPT2 expression and macrophage infiltration. Paired and sequential pretreatment and posttreatment tumor biopsies were stained with anti-ANGPT2, anti-CD68, and anti-CD163, respectively. **A,** ANGPT2 upregulation was accompanied by increased infiltration of $CD68^+$ and $CD163^+$ macrophages in posttreatment tumor of an ipilimumab-treated patient. **B** and **C,** ANGPT2 downregulation and upregulation in posttreatment tumor vasculature of ipilimumab plus bevacizumab-treated patients was respectively accompanied by decreased and increased infiltration of $CD68^+$ and $CD163^+$ macrophages. **D** and **E,** Semiquantitative analysis of macrophage infiltration in tumors with increased (**D**, $n = 4$) and decreased (**E**, $n = 3$) vascular ANGPT2 expression.

by the treatment (Supplementary Table S4), suggesting that other chemoattractants (such as CXCL12 and CCL2) may also be involved in tumor macrophage recruitment (31, 39), as well as inherent sampling bias and heterogeneity associated with human sample collection.

ANGPT2 upregulates PD-L1 expression on M2-polarized macrophages

The association of serum ANGPT2 concentration and clinical outcomes to immune checkpoint therapy suggested that ANGPT2 may play additional roles in immune regulation. We thus examined the effect of ANGPT2 on PD-L1 expression on MDMs that were activated with CSF1, IL4, or IL10 (40–42). CSF1, IL4, and IL10-activated MDMs were derived from normal donors (described in Materials and Methods) and expressed M2 marker CD163, no or low M1 marker CD80 (Supplementary Fig. S4A), and have been shown to have prometastatic, proangiogenic, and immunosuppressive activities (40, 41, 43). ANGPT2 increased PD-L1 expression on CSF1, IL10, and IL4-activated macrophages (Fig. 5A–C). This effect was somewhat heterogeneous in magnitude among donors (Supplementary Fig. S4B and S4C).

Immune checkpoint therapy elicited antibody responses to ANGPT2

Ipilimumab plus bevacizumab can elicit humoral immune responses to target antigens in patients with advanced melanoma (3, 34). Therefore, we investigated antibody responses to ANGPT2 in patients receiving ipilimumab, ipilimumab plus bevacizumab, and PD-1 blockade using immunoblot analyses and ELISA. ANGPT2 antibody concentrations in the pretreatment and posttreatment plasma samples of representative ipilimumab plus bevacizumab-treated patients were measured (Fig. 6A and B). Approximately 8%, 19%, and 21% of the patients, including responders and nonresponders (Supplementary Fig. S5A–S5C), displayed an increase in the ANGPT2 antibody level by 40% or more in response to PD-1 blockade, ipilimumab, and ipilimumab plus bevacizumab, respectively (Fig. 6C). Robust ANGPT2 antibody increases were detected in two ipilimumab plus bevacizumab-treated patients (P16 and P26) who survived for more than 3 years with stable disease (Fig. 6A, B and D). Of note, the increase in ANGPT2 antibody appeared to parallel a rise in circulating ANGPT2 in patient P26 (Fig. 6D). A significant ANGPT2 antibody increase was

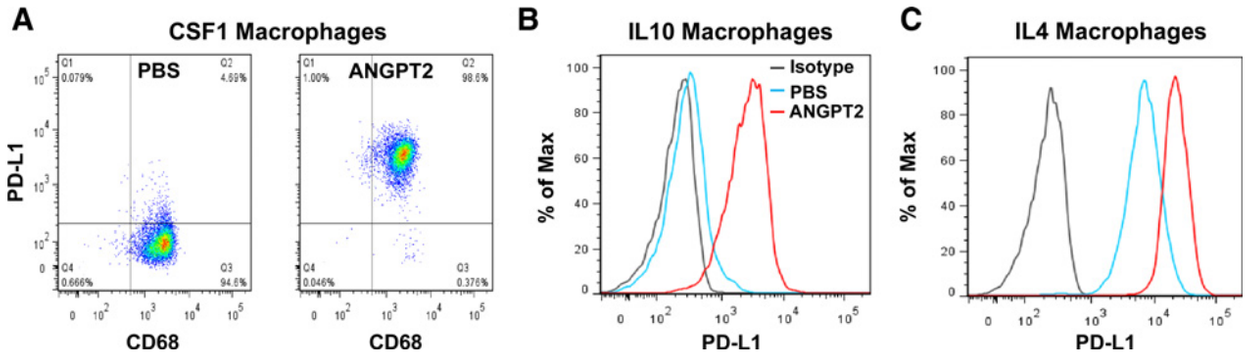

Figure 5.

ANGPT2 induces PD-L1 expression on M2-polarized MDMs. **A–C,** MDMs were differentiated from monocytes with CSF1 and then treated with ANGPT2 (300 ng/mL) for 3 days in the presence of CSF1 (**A**) or for 2 days in the presence of IL10 (**B**) or IL4 (**C**). MDMs were sequentially stained with PE-conjugated PD-L1 antibody and FITC-conjugated CD68 antibody. Macrophages were gated on forward scatter/side scatter and analyzed for CD68 and PD-L1 expression (**A**) or gated on $CD68^+$ cells and analyzed for PD-L1 expression (**B** and **C**). Representative results of at least 4 independent experiments are shown.

also observed in a long-term responder of ipilimumab (Fig. 6E) and PD-1 blockade (Fig. 6F). Longitudinal analyses revealed that ANGPT2 antibody levels increased following initial treatment and lasted for months to years (Fig. 6D–F). To determine the functionality of the endogenous ANGPT2 antibodies, we purified ANGPT2 antibodies from the posttreatment plasma of patient P26 using ANGPT2 coupled beads (detailed protocols are provided in Materials and Methods). The enriched antibodies

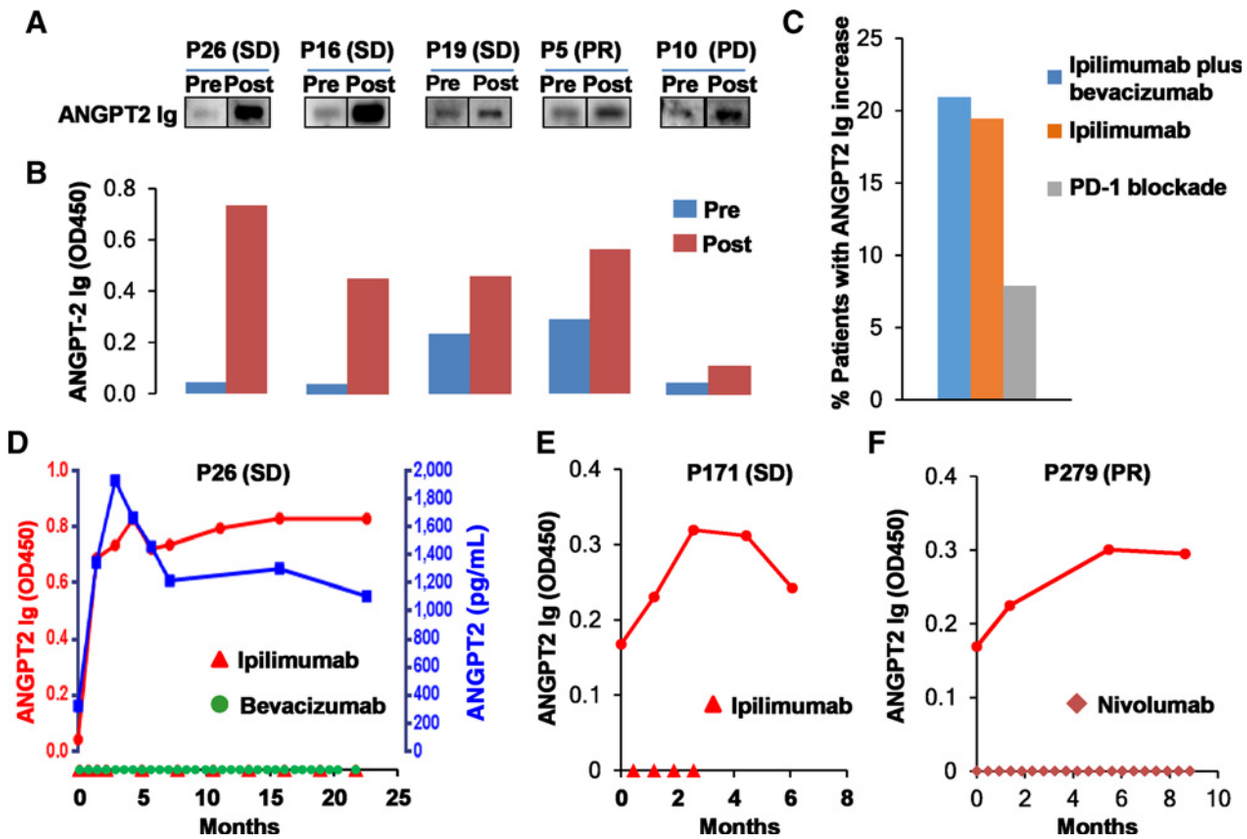

Figure 6.

Immune checkpoint therapy elicited antibody responses to ANGPT2. **A** and **B,** ANGPT2 antibodies were detected in pretreatment and posttreatment plasma samples of ipilimumab plus bevacizumab-treated patients by immunoblot analysis (**A**) and ELISA (**B**). Clinical responses are also indicated. **C,** Proportions of patients receiving ipilimumab plus bevacizumab ($n = 43$), ipilimumab ($n = 36$), and PD-1 blockade ($n = 38$) displayed an increase by 40% or more in ANGPT2 antibody concentrations. **D–F,** Longitudinal analysis of serum ANGPT2 and/or ANGPT2 antibodies in patients receiving ipilimumab plus bevacizumab (**D**), ipilimumab (**E**), or PD-1 blockade (**F**). Dosing of ipilimumab, bevacizumab, or nivolumab was indicated on the *x*-axis. Day 0 is pretreatment.

recognized ANGPT2 and inhibited ANGPT2-mediated Erk1/2 phosphorylation in HUVEC (Supplementary Fig. S6A and S6B), demonstrating their capability of neutralizing the biological activity of ANGPT2.

Discussion

Identification of predictive and prognostic biomarkers as well as mechanisms of resistance to immune therapy will help not only in selecting patients who may benefit from treatment but also in finding combinatorial approaches that offer hope for improved patient outcomes. We report that both high pretreatment concentrations and increases in serum ANGPT2 early during treatment were associated with reduced survival and/or response in patients receiving immune checkpoint blockade. Although previous studies have identified serum ANGPT2 as a prognostic biomarker for a number of types of cancers, including melanoma and colon cancer being treated with anti-VEGF containing therapy (23–27), the current observations suggest that pretreatment serum ANGPT2 concentration, ANGPT2 fold change, and their combination can potentially be used as a prognostic and/or predictive biomarker for immune checkpoint therapy.

Predictive and prognostic biomarker candidates for checkpoint blockade have been difficult to reliably validate. Recent candidates have included tumor and immune cell PD-L1 expression for anti–PD-1/PD-L1 therapy in many tumor types, as well as the significance of a preexisting inflamed tumor microenvironment to predict clinical benefit (44). Tumor heterogeneity and the focal and dynamic nature of PD-L1 expression makes such biomarker evaluation challenging (44). Serologic markers may provide a global assessment of immune activation and provide an immediate snapshot in the dynamic process. Serum ANGPT2 can be easily measured and monitored. It could be an additional parameter to consider for prognostic and predictive evaluation of immune checkpoint blockade in conjunction with other factors or on its own. Additional prospective studies to confirm these initial observations are warranted as well as further understanding of the complex biology influencing patient outcomes to treatment.

ANGPT2 is well known to have proangiogenic and protumoral activity, as well as function in resistance to anti-VEGF therapy (20–22, 32, 45). The association of serum ANGPT2 level with poor clinical outcomes to immune checkpoint therapy suggests that ANGPT2 may also contribute to resistance to immune checkpoint therapy. This may be attributed to its role in the recruitment of monocytes/macrophages into the tumor microenvironment and induction of PD-L1 expression in M2-polarized macrophages. We observed an association of tumor vascular ANGPT2 expression and macrophage infiltration in patient tumors, suggesting that tumor vascular ANGPT2 may play a significant role in tumor macrophage recruitment. This is consistent with previous findings from animal studies that tumor-derived ANGPT2 and endothelial cell–specific overexpression of ANGPT2 promote tumor recruitment of macrophages (28, 29, 45, 46). In addition, we showed that ANGPT2 promoted PD-L1 expression on M2-polarized macrophages. Tumor-associated macrophages (TAM) promote tumor initiation, invasion, metastasis, angiogenesis, and immune suppression (47). High TAM infiltration correlates with a poor prognosis in most human tumor types (48–50). Specifically, PD-L1$^+$ monocytes/macrophages effectively suppress tumor-specific T-cell immunity, and tumor infiltration of PD-L1$^+$ monocytes/macrophages is associated with disease progression and reduced survival in patients (51). Because PD-1 blockade and ipilimumab target distinct immune checkpoints and act on different stages of T-cell activation, upregulation of PD-L1 may confer resistance to ipilimumab-based therapy and limit effectiveness of PD-1 or PD-L1 directed treatment. These studies together may suggest a critical role for ANGPT2 in TAM recruitment and in shaping the proangiogenic and immunosuppressive environment of tumors.

The potential role of ANGPT2 in resistance to anti–CTLA-4 or anti–PD-1 therapy is also supported by the ipilimumab and PD-1 blockade–induced increase in serum ANGPT2 in substantial proportions of the nonresponders. Increased ANGPT2 expression in tumors was also observed in ipilimumab-treated patients. Ipilimumab plus bevacizumab decreased ANGPT2 expression in sera and in tumors, most pronounced in the tumor vasculature. Together with the *in vitro* data, these findings reveal an important role for VEGF in upregulation of tumor vascular ANGPT2 expression, and prevention of such expression by bevacizumab, leading to decreased endothelial ANGPT2 expression. This mechanism may prevent infiltration of M2 macrophages into tumors. Such a phenomenon is in agreement with animal studies showing that dual inhibition of VEGF and ANGPT2 led to reprogramming of macrophages in glioblastoma (52, 53). Anti-VEGF may also reduce ANGPT2 expression in tumor cells by normalizing tumor vessels and making the tumor microenvironment less hypoxic. Anti-VEGF may reduce tumor vascular ANGPT2 expression at least with initial treatment, thereby further contributing to the antitumor effect of immune therapy. In addition, the ANGPT2-resistant mechanism for anti-VEGF therapy may be a long-term consequence and not significant during initiation of therapy.

Extending our previous findings (3, 34), we demonstrated that immune checkpoint therapy elicited humoral immune responses to ANGPT2. These responses were long lasting and robust in several long-term survivors experiencing clinical benefit. ANGPT2 antibodies induced by immune therapy are functional in neutralization of biological activity of ANGPT2 (30). Together with the antitumor effect of ANGPT2 antibodies observed in animal studies and clinical trials (54–57), antibody responses to ANGPT2 may potentially contribute to the antitumor activity of immune checkpoint therapy, suggesting the need for further investigation.

In summary, serum ANGPT2 may be used as a prognostic and/or predictive biomarker for immune checkpoint therapy. ANGPT2 may constitute a resistance mechanism for immune checkpoint therapy by enhancing tumor recruitment of monocytes/macrophages and upregulating PD-L1 expression in TAM. Additionally, reduction in tumor vascular ANGPT2 expression by anti-VEGF and antibody responses to ANGPT2 elicited by immune checkpoint blockade may enhance efficacy of immune therapy. Therefore, ANGPT2 should be considered a pertinent target for therapeutic intervention particularly in combination with immune checkpoint blockade. These findings may have immediate clinical implications for improving the efficacy of current and developing cancer treatments.

Disclosure of Potential Conflicts of Interest

X. Wu, J. Zhou, and FS. Hodi have interest in Angiopoietin-2 Biomarkers Predictive of Anti-Immune Checkpoint Response, per institution policy (patent

application is pending). D.F. McDermott is a consultant/advisory board member for Bristol-Myers-Squibb. S.J. Rodig reports receiving a commercial research grant from Bristol-Myers-Squibb, has received speakers bureau honoraria from Bristol-Myers-Squibb, and is a consultant/advisory board member for Perkin-Elmer. F.S. Hodi reports receiving a commercial research grant from Bristol-Myers Squibb, has ownership interest in MICA related disorders patent pending to institution per institutional policy and antigen targets and uses thereof patent per institutional policy, and is a consultant/advisory board member for Merck, Novartis, Genentech, and EMD Serono. No potential conflicts of interest were disclosed by the other authors.

Authors' Contributions

Conception and design: X. Wu, F.S. Hodi
Development of methodology: X. Wu, X. Liao, C. Connelly, E.M. Connolly, J. Li, M. Severgnini, S. Rodig, F.S. Hodi
Acquisition of data (provided animals, acquired and managed patients, provided facilities, etc.): X. Wu, X. Liao, C. Connelly, E.M. Connolly, J. Li, M.P. Manos, D. Lawrence, D. McDermott, M. Severgnini, A. Lako, M. Lipschitz, C.J. Pak, S. Abdelrahman, S. Rodig, F.S. Hodi
Analysis and interpretation of data (e.g., statistical analysis, biostatistics, computational analysis): X. Wu, A. Giobbie-Hurder, X. Liao, E. Gjini, A. Lako, M. Lipschitz, S. Rodig, F.S. Hodi
Writing, review, and/or revision of the manuscript: X. Wu, A. Giobbie-Hurder, X. Liao, E.M. Connolly, D. Lawrence, D. McDermott, J. Zhou, F.S. Hodi
Administrative, technical, or material support (i.e., reporting or organizing data, constructing databases): M.P. Manos, D. Lawrence, C.J. Pak, S. Abdelrahman, F.S. Hodi
Study supervision: D. Lawrence, S. Rodig, F.S. Hodi

Grant Support

This study was supported by NIHCA143832 (F.S. Hodi), the Melanoma Research Alliance (F.S. Hodi), the Sharon Crowley Martin Memorial Fund for Melanoma Research (F.S. Hodi) and the Malcolm and Emily Mac Naught Fund for Melanoma Research (F.S. Hodi) at Dana-Farber Cancer Institute, Genentech/Roche, and Bristol-Myers Squibb. This study was also supported by a Stand Up To Cancer – Cancer Research Institute Cancer Immunology Dream Team Translational Research Grant (SU2C-AACR-DT1012). Stand Up To Cancer is a program of the Entertainment Industry Foundation administered by the American Association for Cancer Research.

The costs of publication of this article were defrayed in part by the payment of page charges. This article must therefore be hereby marked *advertisement* in accordance with 18 U.S.C. Section 1734 solely to indicate this fact.

Received August 12, 2016; revised November 7, 2016; accepted November 9, 2016; published OnlineFirst December 21, 2016.

References

1. Hodi FS, O'Day SJ, McDermott DF, Weber RW, Sosman JA, Haanen JB, et al. Improved survival with ipilimumab in patients with metastatic melanoma. N Engl J Med 2010;363:711–23.
2. Robert C, Thomas L, Bondarenko I, O'Day S, Weber J, Garbe C, et al. Ipilimumab plus dacarbazine for previously untreated metastatic melanoma. N Engl J Med 2011;364:2517–26.
3. Hodi FS, Lawrence D, Lezcano C, Wu X, Zhou J, Sasada T, et al. Bevacizumab plus ipilimumab in patients with metastatic melanoma. Cancer Immunol Res 2014;2:632–42.
4. Topalian SL, Hodi FS, Brahmer JR, Gettinger SN, Smith DC, McDermott DF, et al. Safety, activity, and immune correlates of anti-PD-1 antibody in cancer. N Engl J Med 2012;366:2443–54.
5. Hamid O, Robert C, Daud A, Hodi FS, Hwu WJ, Kefford R, et al. Safety and tumor responses with lambrolizumab (anti-PD-1) in melanoma. N Engl J Med 2013;369:134–44.
6. Topalian SL, Sznol M, McDermott DF, Kluger HM, Carvajal RD, Sharfman WH, et al. Survival, durable tumor remission, and long-term safety in patients with advanced melanoma receiving nivolumab. J Clin Oncol 2014;32:1020–30.
7. Postow MA, Callahan MK, Wolchok JD. Immune checkpoint blockade in cancer therapy. J Clin Oncol 2015;33:1974–82.
8. Powles T, Eder JP, Fine GD, Braiteh FS, Loriot Y, Cruz C, et al. MPDL3280A (anti-PD-L1) treatment leads to clinical activity in metastatic bladder cancer. Nature 2014;515:558–62.
9. Ansell SM, Lesokhin AM, Borrello I, Halwani A, Scott EC, Gutierrez M, et al. PD-1 blockade with nivolumab in relapsed or refractory Hodgkin's lymphoma. N Engl J Med 2015;372:311–9.
10. Wolchok JD, Kluger H, Callahan MK, Postow MA, Rizvi NA, Lesokhin AM, et al. Nivolumab plus ipilimumab in advanced melanoma. N Engl J Med 2013;369:122–33.
11. Postow MA, Chesney J, Pavlick AC, Robert C, Grossmann K, McDermott D, et al. Nivolumab and ipilimumab versus ipilimumab in untreated melanoma. N Engl J Med 2015;372:2006–17.
12. Larkin J, Chiarion-Sileni V, Gonzalez R, Grob JJ, Cowey CL, Lao CD, et al. Combined nivolumab and ipilimumab or monotherapy in untreated melanoma. N Engl J Med 2015;373:23–34.
13. Rivera LB, Bergers G. Intertwined regulation of angiogenesis and immunity by myeloid cells. Trends Immunol 2015;36:240–9.
14. Ohm JE, Carbone DP. VEGF as a mediator of tumor-associated immunodeficiency. Immunol Res 2001;23:263–72.
15. Oyama T, Ran S, Ishida T, Nadaf S, Kerr L, Carbone DP, et al. Vascular endothelial growth factor affects dendritic cell maturation through the inhibition of nuclear factor-kappa B activation in hemopoietic progenitor cells. J Immunol 1998;160:1224–32.
16. Vanneman M, Dranoff G. Combining immunotherapy and targeted therapies in cancer treatment. Nat Rev Cancer 2012;12:237–51.
17. Shrimali RK, Yu Z, Theoret MR, Chinnasamy D, Restifo NP, Rosenberg SA. Antiangiogenic agents can increase lymphocyte infiltration into tumor and enhance the effectiveness of adoptive immunotherapy of cancer. Cancer Res 2010;70:6171–80.
18. Huang H, Langenkamp E, Georganaki M, Loskog A, Fuchs PF, Dieterich LC, et al. VEGF suppresses T-lymphocyte infiltration in the tumor microenvironment through inhibition of NF-kappaB-induced endothelial activation. FASEB J 2015;29:227–38.
19. Yuan J, Zhou J, Dong Z, Tandon S, Kuk D, Panageas KS, et al. Pretreatment serum VEGF is associated with clinical response and overall survival in advanced melanoma patients treated with ipilimumab. Cancer Immunol Res 2014;2:127–32.
20. Fiedler U, Augustin HG. Angiopoietins: a link between angiogenesis and inflammation. Trends Immunol 2006;27:552–8.
21. Huang H, Bhat A, Woodnutt G, Lappe R. Targeting the ANGPT-TIE2 pathway in malignancy. Nat Rev Cancer 2010;10:575–85.
22. Tait CR, Jones PF. Angiopoietins in tumours: the angiogenic switch. J Pathol 2004;204:1–10.
23. Thurston G, Daly C. The complex role of angiopoietin-2 in the angiopoietin-tie signaling pathway. Cold Spring Harb Perspect Med 2012;2:a006550.
24. Helfrich I, Edler L, Sucker A, Thomas M, Christian S, Schadendorf D, et al. Angiopoietin-2 levels are associated with disease progression in metastatic malignant melanoma. Clin Cancer Res 2009;15:1384–92.
25. Jary M, Vernerey D, Lecomte T, Dobi E, Ghiringhelli F, Monnien F, et al. Prognostic value of angiopoietin-2 for death risk stratification in patients with metastatic colorectal carcinoma. Cancer Epidemiol Biomarkers Prev 2015;24:603–12.
26. Dreikhausen L, Blank S, Sisic L, Heger U, Weichert W, Jager D, et al. Association of angiogenic factors with prognosis in esophageal cancer. BMC Cancer 2015;15:121.
27. Goede V, Coutelle O, Neuneier J, Reinacher-Schick A, Schnell R, Koslowsky TC, et al. Identification of serum angiopoietin-2 as a biomarker for clinical outcome of colorectal cancer patients treated with bevacizumab-containing therapy. Br J Cancer 2010;103:1407–14.
28. Scholz A, Lang V, Henschler R, Czabanka M, Vajkoczy P, Chavakis E, et al. Angiopoietin-2 promotes myeloid cell infiltration in a beta(2)-integrin-dependent manner. Blood 2011;118:5050–9.

29. Scholz A, Plate KH, Reiss Y. Angiopoietin-2: a multifaceted cytokine that functions in both angiogenesis and inflammation. Ann NY Acad Sci 2015;1347:45–51.
30. Schoenfeld J, Jinushi M, Nakazaki Y, Wiener D, Park J, Soiffer R, et al. Active immunotherapy induces antibody responses that target tumor angiogenesis. Cancer Res 2010;70:10150–60.
31. Huang H, Lai JY, Do J, Liu D, Li L, Del Rosario J, et al. Specifically targeting angiopoietin-2 inhibits angiogenesis, Tie2-expressing monocyte infiltration, and tumor growth. Clin Cancer Res 2011;17:1001–11.
32. Rigamonti N, Kadioglu E, Keklikoglou I, Wyser Rmili C, Leow CC, De Palma M. Role of angiopoietin-2 in adaptive tumor resistance to VEGF signaling blockade. Cell Rep 2014;8:696–706.
33. Daly C, Eichten A, Castanaro C, Pasnikowski E, Adler A, Lalani AS, et al. Angiopoietin-2 functions as a Tie2 agonist in tumor models, where it limits the effects of VEGF inhibition. Cancer Res 2013;73:108–18.
34. Wu X, Giobbie-Hurder A, Liao X, Lawrence D, McDermott D, Zhou J, et al. VEGF Neutralization Plus CTLA-4 Blockade Alters Soluble and Cellular Factors Associated with Enhancing Lymphocyte Infiltration and Humoral Recognition in Melanoma. Cancer Immunol Res 2016;4:858–68.
35. Wu X, Marmarelis ME, Hodi FS. Activity of the heat shock protein 90 inhibitor ganetespib in melanoma. PLoS One 2013;8:e56134.
36. Contal C, O'Quigley J. An application of changepoint methods in studying the effect of age on survival in breast cancer. Comput Stat Data Anal 1999;30:253–70.
37. Garcia S, Krausz S, Ambarus CA, Fernandez BM, Hartkamp LM, van Es IE, et al. Tie2 signaling cooperates with TNF to promote the pro-inflammatory activation of human macrophages independently of macrophage functional phenotype. PLoS One 2014;9:e82088.
38. Forget MA, Voorhees JL, Cole SL, Dakhlallah D, Patterson IL, Gross AC, et al. Macrophage colony-stimulating factor augments Tie2-expressing monocyte differentiation, angiogenic function, and recruitment in a mouse model of breast cancer. PLoS One 2014;9:e98623.
39. Srivastava K, Hu J, Korn C, Savant S, Teichert M, Kapel SS, et al. Postsurgical adjuvant tumor therapy by combining anti-angiopoietin-2 and metronomic chemotherapy limits metastatic growth. Cancer Cell 2014;26:880–95.
40. Zajac E, Schweighofer B, Kupriyanova TA, Juncker-Jensen A, Minder P, Quigley JP, et al. Angiogenic capacity of M1- and M2-polarized macrophages is determined by the levels of TIMP-1 complexed with their secreted proMMP-9. Blood 2013;122:4054–67.
41. Martinez FO, Gordon S. The M1 and M2 paradigm of macrophage activation: time for reassessment. F1000Prime Rep 2014;6:13.
42. Vogel DY, Glim JE, Stavenuiter AW, Breur M, Heijnen P, Amor S, et al. Human macrophage polarization in vitro: maturation and activation methods compared. Immunobiology 2014;219:695–703.
43. Mantovani A, Sica A. Macrophages, innate immunity and cancer: balance, tolerance, and diversity. Curr Opin Immunol 2010;22:231–7.
44. Mahoney KM, Freeman GJ, McDermott DF. The next immune-checkpoint inhibitors: PD-1/PD-L1 blockade in melanoma. Clin Ther 2015;37:764–82.
45. Coffelt SB, Tal AO, Scholz A, De Palma M, Patel S, Urbich C, et al. Angiopoietin-2 regulates gene expression in TIE2-expressing monocytes and augments their inherent proangiogenic functions. Cancer Res 2010;70:5270–80.
46. Scholz A, Harter PN, Cremer S, Yalcin BH, Gurnik S, Yamaji M, et al. Endothelial cell-derived angiopoietin-2 is a therapeutic target in treatment-naive and bevacizumab-resistant glioblastoma. EMBO Mol Med 2015;8:39–57.
47. Noy R, Pollard JW. Tumor-associated macrophages: from mechanisms to therapy. Immunity 2014;41:49–61.
48. De Palma M, Lewis CE. Macrophage regulation of tumor responses to anticancer therapies. Cancer Cell 2013;23:277–86.
49. Riabov V, Gudima A, Wang N, Mickley A, Orekhov A, Kzhyshkowska J. Role of tumor associated macrophages in tumor angiogenesis and lymphangiogenesis. Front Physiol 2014;5:75.
50. Ostuni R, Kratochvill F, Murray PJ, Natoli G. Macrophages and cancer: from mechanisms to therapeutic implications. Trends Immunol 2015;36:229–39.
51. Kuang DM, Zhao Q, Peng C, Xu J, Zhang JP, Wu C, et al. Activated monocytes in peritumoral stroma of hepatocellular carcinoma foster immune privilege and disease progression through PD-L1. J Exp Med 2009;206:1327–37.
52. Kloepper J, Riedemann L, Amoozgar Z, Seano G, Susek K, Yu V, et al. Ang-2/VEGF bispecific antibody reprograms macrophages and resident microglia to anti-tumor phenotype and prolongs glioblastoma survival. Proc Natl Acad Sci USA 2016;113:4476–81.
53. Peterson TE, Kirkpatrick ND, Huang Y, Farrar CT, Marijt KA, Kloepper J, et al. Dual inhibition of Ang-2 and VEGF receptors normalizes tumor vasculature and prolongs survival in glioblastoma by altering macrophages. Proc Natl Acad Sci USA 2016;113:4470–5.
54. Kienast Y, Klein C, Scheuer W, Raemsch R, Lorenzon E, Bernicke D, et al. Ang-2-VEGF-A CrossMab, a novel bispecific human IgG1 antibody blocking VEGF-A and Ang-2 functions simultaneously, mediates potent antitumor, antiangiogenic, and antimetastatic efficacy. Clin Cancer Res 2013;19:6730–40.
55. Herbst RS, Hong D, Chap L, Kurzrock R, Jackson E, Silverman JM, et al. Safety, pharmacokinetics, and antitumor activity of AMG 386, a selective angiopoietin inhibitor, in adult patients with advanced solid tumors. J Clin Oncol 2009;27:3557–65.
56. Thomas M, Kienast Y, Scheuer W, Bahner M, Kaluza K, Gassner C, et al. A novel angiopoietin-2 selective fully human antibody with potent anti-tumoral and anti-angiogenic efficacy and superior side effect profile compared to Pan-Angiopoietin-1/-2 inhibitors. PLoS One 2013;8:e54923.
57. Mazzieri R, Pucci F, Moi D, Zonari E, Ranghetti A, Berti A, et al. Targeting the ANG2/TIE2 axis inhibits tumor growth and metastasis by impairing angiogenesis and disabling rebounds of proangiogenic myeloid cells. Cancer Cell 2011;19:512–26.